Histidine 332 of the D1 Polypeptide Modulates the Magnetic and Redox Properties of the Manganese Cluster and Tyrosine Y_Z in Photosystem II†

Richard J. Debus,*,‡ Kristy A. Campbell,§ Jeffrey M. Peloquin,§ Donna P. Pham,‡ and R. David Britt*,§

Department of Biochemistry, University of California, Riverside, California 92521-0129, and Department of Chemistry, University of California, Davis, California 95616

Received July 29, 1999; Revised Manuscript Received October 25, 1999

ABSTRACT: An electron spin−echo envelope modulation study [Tang, X.-S., Diner, B. A., Larsen, B. S., Gilchrist, M. L., Jr., Lorigan, G. A., and Britt, R. D. (1994) *Proc. Natl. Acad. Sci. U.S.A. 91*, 704−708] and a recent Fourier transform infrared study [Noguchi, T., Inoue, Y., and Tang, X.-S. (1999) *Biochemistry 38*, 10187−10195], both conducted with [^{15}N]histidine-labeled photosystem II particles, show that at least one histidine residue coordinates the O_2-evolving Mn cluster in photosystem II. Evidence obtained from site-directed mutagenesis studies suggests that one of these residues may be His332 of the D1 polypeptide. The mutation D1-H332E is of particular interest because cells of the cyanobacterium *Synechocystis* sp. PCC 6803 that contain this mutation evolve no O_2 but appear to assemble Mn clusters in nearly all photosystem II reaction centers [Chu, H.-A., Nguyen, A. P., and Debus, R. J. (1995) *Biochemistry 34*, 5859−5882]. Photosystem II particles isolated from the *Synechocystis* D1-H332E mutant are characterized in this study. Intact D1-H332E photosystem II particles exhibit an altered S_2 state multiline EPR signal that has more hyperfine lines and narrower splittings than the S_2 state multiline EPR signal observed in wild-type* PSII particles. However, the quantum yield for oxidizing the S_1 state Mn cluster is very low, corresponding to an 8000-fold slowing of the rate of Mn oxidation by $Y_Z^\bullet$, and the temperature threshold for forming the S_2 state is approximately 100 K higher than in wild-type PSII preparations. Furthermore, the D1-H332E PSII particles are unable to advance beyond the $Y_Z^\bullet S_2$ state, as shown by the accumulation of a narrow "split" EPR signal under multiple turnover conditions. In Mn-depleted photosystem II particles, charge recombination between $Q_A^{\bullet-}$ and $Y_Z^\bullet$ in D1-H332E is accelerated in comparison to wild-type*, showing that the mutation alters the redox properties of Y_Z in addition to those of the Mn cluster. These results are consistent with D1-His332 being located near the Mn−Y_Z complex and perhaps ligating Mn.

Photosynthetic water oxidation takes place in photosystem II (PSII)[1] near the lumenal surface of the thylakoid membrane. PSII is a multisubunit, integral membrane protein complex (*1*, *2*) that utilizes light energy to oxidize water and reduce plastoquinone (for review, see refs *3*−*10*). The oxygen-evolving catalytic site contains four Mn ions that are arranged as a magnetically coupled tetramer (*11*, *12*). This tetrameric Mn cluster accumulates oxidizing equivalents in response to photochemical events within PSII, and then catalyzes the oxidation of two water molecules, releasing one molecule of O_2 as a byproduct.

The photochemical events that precede water oxidation take place in a heterodimer of two homologous polypeptides known as D1 and D2. These events are initiated by the capture of light by an antenna complex that is located peripherally to PSII. The excitation energy is transferred to the photochemically active chlorophyll species known as P_{680}. Excitation of P_{680} results in formation of the charge-separated state, $P_{680}^{\bullet+}Q_A^{\bullet-}$, where Q_A is a molecule of plastoquinone. The $P_{680}^{\bullet+}$ radical rapidly oxidizes tyrosine Y_Z (Tyr161 of the D1 polypeptide), forming the neutral radical, $Y_Z^\bullet$. This radical in turn oxidizes the Mn cluster, while $Q_A^{\bullet-}$ reduces the secondary plastoquinone, Q_B. Subsequent charge-separations result in further oxidation of the Mn cluster. During each catalytic cycle, the Mn cluster cycles through five oxidation states termed S_n, where *n* denotes the number of oxidizing equivalents stored. The S_1 state predominates in dark-adapted samples. The S_3 state may have 1 oxidizing equivalent localized on a Mn ligand: whether Mn is oxidized during the $S_2 \rightarrow S_3$ transition is currently under debate (e.g.,

† This work was supported by the National Institutes of Health (GM43496 to R.J.D. and GM48242 to R.D.B.) and by the National Science Foundation (MCB 9513648 to R.D.B.). A fellowship from the Department of Chemistry at UC Davis and A. A. Jungerman is gratefully acknowledged by K.A.C.

* To whom correspondence should be addressed. R.J.D.: phone (909) 787-3483, fax (909) 787-4434, e-mail debusrj@citrus.ucr.edu. R.D.B.: phone (530) 752-6377, fax (530) 752-8995, e-mail rdbritt@ucdavis.edu.

‡ University of California, Riverside.

§ University of California, Davis.

[1] Abbreviations: Chl, chlorophyll *a*; Car, carotenoid; Chl_Z, monomeric Chl species that is oxidized by $P_{680}^{\bullet+}$, probably via a molecule of carotenoid; DCMU, 3-(3,4-dichlorophenyl)-1,1-dimethylurea; DMSO, dimethyl sulfoxide; EPR, electron paramagnetic resonance; ENDOR, electron nuclear double resonance; ESEEM, electron spin−echo envelope modulation; fwhm, full width at half-maximum; PSII, photosystem II; PPBQ, phenyl-1,4-benzoquinone; P_{680}, chlorophyll species that serves as the light-induced electron donor in PSII; Y_Z, tyrosine residue that mediates electron transfer between the Mn cluster and $P_{680}^{\bullet+}$; Q_A, primary plastoquinone electron acceptor; MES, 2-(*N*-morpholino)ethanesulfonic acid; wild-type*, control strain of *Synechocystis* sp. PCC 6803 constructed in identical fashion as the D1-H332E mutant, but containing the wild-type *psb*A-2 gene.

10.1021/bi9917737 CCC: $19.00
Published on Web 12/08/1999

see ref *13* versus ref *14*). The S_4 state is a transient intermediate that reverts to the S_0 state with the concomitant release of O_2. Simulations of EPR and ENDOR data obtained with samples trapped in the $S_2Y_Z^{\bullet}$ state show that the point−dipole distance between $Y_Z^{\bullet}$ and the Mn cluster is 7−9 Å (*12*, *15*, *16*) (also see refs *17* and *125*). This point−dipole distance is compatible with recent models for O_2 formation that invoke proton-coupled electron transfer from Mn-bound substrate water molecules to $Y_Z^{\bullet}$ during some or all of the S state transitions (*4*, *18*−*24*). This 7−9 Å point−dipole distance is compatible with direct hydrogen bonding between Y_Z and Mn-bound substrate water molecules (*9*, *21*, *22*) but is equally compatible with indirect hydrogen bonding, such as via an intervening water molecule (*24*).

Several lines of evidence suggest that the D1 polypeptide contributes most or all of the amino acid residues that coordinate the Mn and Ca^{2+} ions in PSII (for review, see refs *3*, *4*, *10*). The Mn ions are believed to be coordinated primarily by carboxylate residues. Coordination by both carboxylate and histidine residues has been proposed on the basis of chemical modification studies (*25*−*33*). Coordination by at least one histidine residue has been demonstrated by ESEEM (*34*) and FTIR (*35*) studies conducted with PSII particles labeled with [^{15}N]histidine. Coordination by a carboxylate residue that forms a bridge to a Ca^{2+} ion has been proposed on the basis of an FTIR study that compared the S_2-*minus*-S_1 difference spectrum of intact and Ca^{2+}-depleted samples (*36*). Site-directed mutagenesis studies have identified D1-Asp170 (*37*−*41*), D1-His190 (*41*−*44*), D1-His332 (*42*, *44*, *45*), D1-Glu333 (*42*, *44*, *45*), D1-His337 (*42*, *44*, *45*), D1-Asp342 (*42*, *44*, *45*), and the *C*-terminus of Ala344 (*46*) as potential ligands of the Mn cluster (for review, see refs *4*, *10*). The residue D1-His337 has also been proposed to ligate the Mn cluster on the basis of chemical modification and protease digestion studies (*28*, *33*).

The ESEEM (*34*) and FTIR (*35*) studies showing that at least one histidine residue coordinates the Mn cluster in PSII have focused attention on D1-His190, D1-His332, and D1-His337. In this study, we present a characterization of PSII particles isolated from the cyanobacterial mutant D1-H332E. This mutant is of particular interest because it appears to assemble Mn clusters in nearly all reaction centers in vivo, but evolves no O_2 (*45*). In this study, we show that the mutation D1-H332E alters the redox properties of both the Mn cluster and Y_Z and alters the magnetic properties of the Mn cluster.

MATERIALS AND METHODS

Construction of Site-Directed Mutants. The D1-H332E mutation was constructed in the *psbA-2* gene of the cyanobacterium *Synechocystis* sp. PCC 6803 (*39*). The D1-H332E mutant strain containing PSI was described previously (*45*). To simplify the isolation of PSII particles, the plasmid bearing the D1-H332E mutation was also transformed into a strain of *Synechocystis* that lacks PSI and *apc*E function (*47*). The wild-type* strains were constructed in an identical fashion as the mutants except that the transforming plasmid carried no site-directed mutation. The designation "wild-type*" differentiates these strains from the native wild-type strain that contains all three *psb*A genes and is sensitive to antibiotics. Wild-type* and D1-H332E cells containing PSI were propagated in the presence of 5 mM glucose (*48*) as described previously (*45*). Wild-type* and D1-H332E cells lacking PSI were propagated in the presence of 15 mM glucose (*49*) as described previously (*50*).

Isolation of PSII Particles. Wild-type* and D1-H332E PSII particles from cells containing PSI were isolated as described by Tang and Diner (*51*) with minor modification (*50*). Wild-type* and D1-H332E PSII particles from cells lacking PSI were isolated as described previously (*50*) except that the detergent-extracted thylakoid membranes were applied to a 300 mL DEAE-Toyopearl 650s column, the column was washed with purification buffer [25% (v/v) glycerol, 50 mM MES−NaOH, 20 mM $CaCl_2$, 5 mM $MgCl_2$, 0.03% *n*-dodecyl β-D-maltoside, pH 6.0], and the purified PSII particles were eluted with purification buffer containing 50 mM $MgSO_4$. The O_2 evolution activity of the wild-type* PSII particles was 5−6 mmol of O_2 (mg of Chl)$^{-1}$ h^{-1}. For Mn-depleted PSII particles, the extraction of Mn was performed with NH_2OH and EDTA as described previously (*50*). The residual O_2 evolution activity of the Mn-depleted wild-type* preparations was ≤5% in comparison to untreated wild-type* PSII particles. Purified PSII particles were concentrated to ≈0.5 mg of Chl/mL by ultrafiltration (*51*), frozen in liquid N_2, and stored at −80 °C. For EPR experiments, PSII particles were further concentrated to 4−5 mg of Chl/mL with Centricon-100 concentrators (Millipore Corp., Bedford, MA).

EPR Measurements. EPR spectra were recorded with a Bruker ECS106 X-band CW-EPR spectrometer equipped with either an ER-4102ST standard mode cavity or an ER-4116DM dual mode cavity. Cryogenic temperatures were obtained with an Oxford ESR900 liquid helium cryostat. The temperature was controlled with an Oxford ITC503 temperature and gas flow controller that was equipped with a gold−iron chromel thermocouple. This thermocouple was calibrated with a carbon glass resistor from 3.6 to 300 K. Samples were illuminated in a non-silvered dewar using a focused 300 W IR-filtered Radiac light source and a Schott 150 W IR-filtered fiber optic lamp and were immediately frozen in liquid N_2 after illumination. For the experiments of Figure 2, samples were illuminated in the presence of DCMU for 1.5 min at 195 K (methanol/dry ice), 231 K (acetonitrile/dry ice), 244 K (*o*-xylene/liquid N_2), 258 K (ethylene glycol/dry ice), or 273 K (ice water). The amplitude of the multiline EPR signal was estimated from the average integrated areas of two low-field and six high-field peaks (marked with asterisks in the inset of Figure 2). The chosen peaks do not overlap with the signal of $Q_A^{\bullet-}$ Fe^{2+}. The area of each peak was determined after base line subtraction between the points delimiting each individual peak.

Optical Measurements. Transient absorbance changes of Y_Z at 287.5 nm ($\Delta A_{287.5}$) and Q_A at 325 nm (ΔA_{325}) were measured with a modified CARY-14 spectrophotometer (On-Line Instrument Systems, Inc., Bogart, GA) operated in the single-beam mode (*50*). The photomultiplier tube was protected by two Corion Solar Blind filters. Actinic flashes (approximately 4 μs fwhm) were provided by a Xenon Corp. (Woburn, MA) model 457A xenon flash-lamp system (0.5 μF capacitor charged to 7−8 kV). The flashes were passed through two 2-mm-thick Schott WG-360 filters, two 2-mm-thick Schott RG-610 filters, and one Corion LS-750 filter and were directed to the sample cuvette with a 3.8-m-long

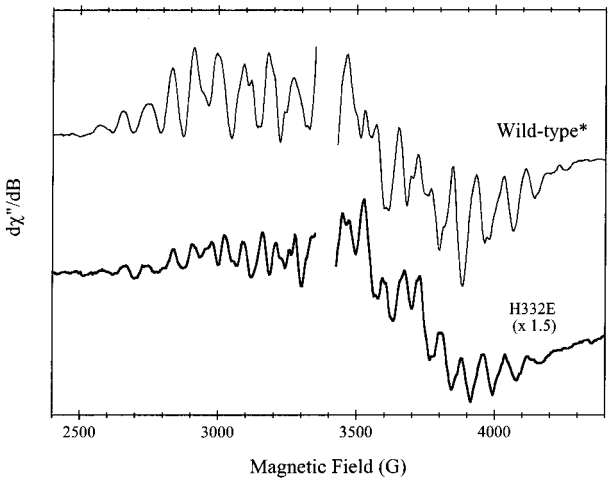

FIGURE 1: Light-*minus*-dark EPR spectrum of wild-type* (upper trace) and D1-H332E (lower trace) PSII particles. Samples [≈5 mg of Chl/mL in 25% (v/v) glycerol, 50 mM MES−NaOH (pH 6.0), 20 mM $CaCl_2$, 5 mM $MgCl_2$, 25 mM $MgSO_4$, 0.03% *n*-dodecyl β-D-maltoside, 1 mM DCMU, 1% (v/v) DMSO] were illuminated for 30 s at 273 K before being flash-frozen in liquid N_2. Experimental conditions: standard mode cavity; microwave frequency, 9.5 GHz; microwave power, 3.2 mW; modulation amplitude, 16 G; modulation frequency, 100 kHz; time constant, 41 ms; conversion time, 82 ms; temperature, 7 K; 25 scans. Both spectra have had the $g = 2.0$ region, containing the EPR signal of $Y_D^{\bullet}$, removed for clarity. To facilitate comparison of spectra, the amplitude of the D1-H332E trace has been multiplied by a factor of 1.5. The PSII particles were isolated from cells containing PSI.

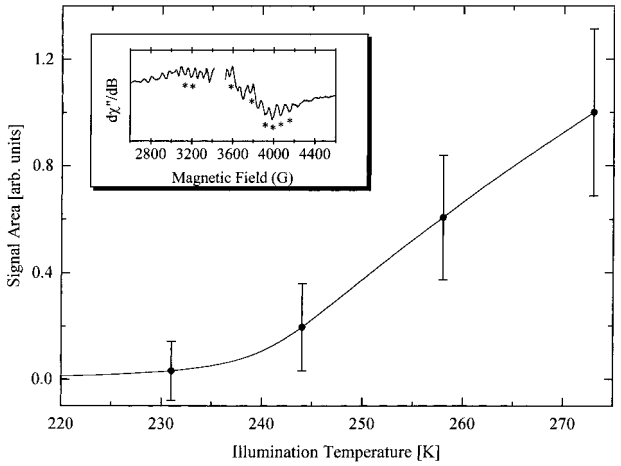

FIGURE 2: Normalized amplitude of the light-*minus*-dark multiline EPR signal of D1-H332E PSII particles as a function of illumination temperature. Samples [≈5 mg of Chl/mL in 25% (v/v) glycerol, 50 mM MES−NaOH (pH 6.0), 20 mM $CaCl_2$, 5 mM $MgCl_2$, 25 mM $MgSO_4$, 0.03% *n*-dodecyl β-D-maltoside, 1 mM DCMU, 1% (v/v) DMSO] were illuminated for 1.5 min at the indicated temperature before being flash-frozen in liquid N_2. The signal amplitudes were estimated from the average integrated areas of two low-field and six high-field peaks (marked with asterisks in the inset) and were normalized to the amplitude estimated at 273 K. The chosen peaks do not overlap with the signal of $Q_A^{\bullet-}$ Fe^{2+}. At each temperature, the area of each peak was determined after base line subtraction between the points delimiting each individual peak. The error bars correspond to the sample standard deviations calculated from the eight individual integrated peak areas. However, all eight peaks showed the same increase in area with temperature. Inset: Light-*minus*-dark multiline EPR signal of D1-H332E PSII particles after illumination at 273 K. The $g = 2.0$ region has been removed for clarity. Experimental conditions: dual mode cavity; microwave frequency, 9.68 GHz; microwave power, 3.2 mW; modulation amplitude, 10 G; modulation frequency, 100 kHz; time constant, 82 ms; conversion time, 41 ms; temperature, 7 K; 15 scans. The PSII particles were isolated from cells lacking PSI.

flexible light guide (Schott Fiber Optics, Southbridge, MA). The cuvette containing the sample was held in a thermostated jacket. For measurements, samples were diluted (10 μg of Chl into 0.5 mL final volume) into purification buffer containing 0.04% *n*-dodecyl β-D-maltoside. To ensure the oxidation of Q_A and Y_D prior to data acquisition, the following procedures were employed. For measurements at 325 nm, samples were incubated in the presence of 10 μM $K_3Fe(CN)_6$ for 2 min, and then given 6 flashes 20 s apart and dark-adapted for another 2 min before DCMU (dissolved in DMSO) was added to 25 μM. The samples were then subjected to 28 flashes spaced 1 min apart. Data acquisition commenced with the fourth flash. For measurements at 287.5 nm, samples were incubated in the presence of 10 μM $K_3Fe(CN)_6$ for 2 min, and then given 154 flashes spaced 10 s apart. Data acquisition commenced with the 11th flash. Kinetics were analyzed with Jandel Scientific's (San Rafael, CA) PeakFit program, version 4.0.

Other Procedures. Chlorophyll *a* concentrations and light-saturated rates of oxygen evolution were measured as described previously (*39*, *50*). When used, PPBQ was purified by sublimation.

RESULTS

EPR Spectra. A multiline EPR signal was observed in D1-H332E PSII particles in perpendicular mode after illumination at 273 K in the presence of DCMU (Figure 1, lower trace). This signal has more hyperfine lines and narrower splittings than the S_2 state multiline EPR signal that is observed in wild-type* PSII particles illuminated under the same conditions (Figure 1, upper trace). The integrated area of the mutant signal was approximately 62% of the integrated area of the wild-type* signal. Because 92 ± 3% of the wild-type* PSII reaction centers were estimated to contain photooxidizable Mn clusters (see below) and because the two samples contained approximately equivalent amounts of chlorophyll, we conclude that approximately 57% of the D1-H332E PSII reaction centers gave rise to the altered multiline EPR signal. We assign this signal to the S_2 state of the Mn cluster in D1-H332E PSII particles because it was generated by illuminating dark-adapted PSII particles in the presence of DCMU, which limits PSII to a single S state advancement. The D1-H332E multiline EPR signal was the same whether the PSII particles were isolated from *Synechocystis* cells containing or lacking PSI (e.g., compare the lower trace of Figure 1 with the inset of Figure 2). The same was true for the wild-type* multiline EPR signal (comparison not shown). The temperature threshold for forming the multiline signal in D1-H332E PSII particles was approximately 100 K higher than is normally observed in wild-type PSII preparations: illumination at 258 K generated only about 50% of the signal generated by illumination at 273 K (Figure 2). In contrast, the multiline signal in wild-type PSII preparations from spinach is half-maximal at 135−150 K (*52*, *53*). Although the temperature threshold for forming the multiline EPR signal in wild-type* PSII particles from *Synechocystis* was not measured, the signal could be generated by illumination at 195 K (not shown). A similar increase in the temperature threshold for forming the S_2 state has been observed in PSII preparations from spinach after treatment

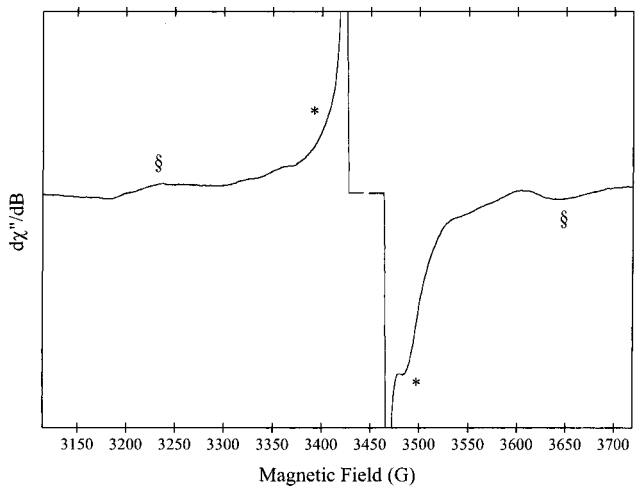

FIGURE 3: Light-*minus*-dark EPR spectrum of the "split" EPR signal of D1-H332E PSII particles. Sample [≈4 mg of Chl/mL in 25% (v/v) glycerol, 50 mM MES−NaOH (pH 6.0), 20 mM $CaCl_2$, 5 mM $MgCl_2$, 50 mM $MgSO_4$, 0.03% *n*-dodecyl β-D-maltoside, 0.6 mM $K_3Fe(CN)_6$, 0.6 mM PPBQ, 1% (v/v) DMSO] was illuminated for 20 s at 273 K before being flash-frozen in liquid N_2. The points marked by asterisks are split by 100 G. The points marked "§" are split by about 410 G. Experimental conditions: dual mode cavity; microwave frequency, 9.68 GHz; microwave power, 3.2 mW; modulation amplitude, 10 G; modulation frequency, 100 kHz; time constant, 82 ms; conversion time, 41 ms; temperature, 7 K; 15 scans. The PSII particles were isolated from cells lacking PSI.

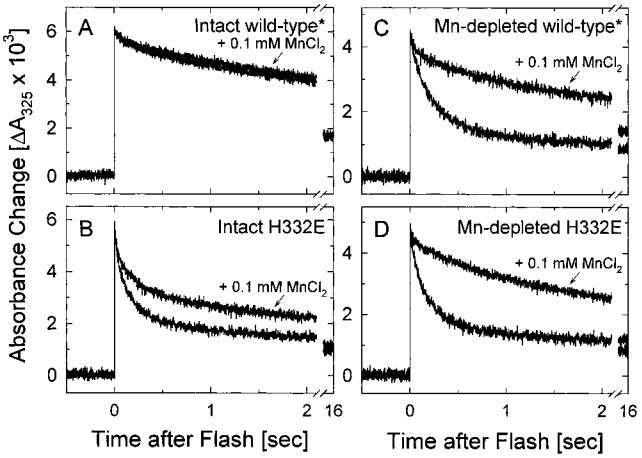

FIGURE 4: Formation and decay of $Q_A^{\bullet-}$ after a single flash applied to intact and Mn-depleted PSII particles in the absence and presence of 0.1 mM $MnCl_2$, as measured at 325 nm. (A) Intact wild-type* PSII particles. Note that the traces obtained in the absence and presence of 0.1 mM $MnCl_2$ nearly overlap. (B) Intact D1-H332E PSII particles. (C) Mn-depleted wild-type* PSII particles. (D) Mn-depleted D1-H332E PSII particles. To facilitate comparisons, the amplitudes of the traces obtained in the presence of $MnCl_2$ were multiplied by factors of 1.04, 1.13, 1.42, and 1.25 in panels A−D, respectively. Experimental conditions: 20 μg of Chl/mL in 25% (v/v) glycerol, 50 mM MES−NaOH (pH 6.0), 20 mM $CaCl_2$, 5 mM $MgCl_2$, 0.04% *n*-dodecyl β-D-maltoside, 10 μM $K_3Fe(CN)_6$, 25 μM DCMU, 1% DMSO, pH 6.0, 294 K. Traces represent the average of 25 sweeps except for those in panels C and D that were obtained in the presence of $MnCl_2$: these traces represent the average of 50 sweeps. Samples were replaced after 25 sweeps.

with acetate (*54*) or depletion of Ca^{2+} (*55*, *56*). In the presence of chelating agents, Ca^{2+}-depleted PSII preparations from spinach also exhibit an altered S_2 state multiline EPR signal (*57*−*61*).

No recognizable Mn EPR signals were produced in D1-H332E PSII particles by illumination at 195 K (not shown). Illumination at this temperature produced only a narrow radical that presumably corresponds to $Chl_Z^{+\bullet}$ (*62*, *63*) and/or $Car^{+\bullet}$ (*64*, *65*) (not shown). Also, no S_1 state parallel-mode multiline EPR signal (*66*, *67*) was observed in intact, dark-adapted D1-H332E PSII particles (not shown).

Illumination of D1-H332E PSII particles at 273 K in the presence of PPBQ and $K_3Fe(CN)_6$ as electron acceptors produced a narrow "split" EPR signal with a line width of ≈100 G and additional features split by ≈410 G (Figure 3). No multiline EPR signal was present under these conditions. The split EPR signal was similar to those observed in Ca^{2+}-depleted (*57*−*61*, *68*), Cl^--depleted (*68*, *69*), and acetate-treated (*17*, *54*, *70*−*72*) PSII preparations from spinach, which are unable to advance beyond the $Y_Z^{\bullet}S_2$ state (*23*, *73*), and in NH_3-treated PSII preparations (*74*, *75*), in which one or more S transitions are slowed (*76*). An inability to advance beyond the $Y_Z^{\bullet}S_2$ state would be consistent with the inability of D1-H332E cells to evolve O_2 despite the apparent presence of Mn clusters (*45*).

Electron-Transfer Kinetics: $Q_A^{\bullet-}$ Oxidation by Mn or $Y_Z^{\bullet}$. To further characterize the Mn clusters in D1-H332E PSII particles, the kinetics of charge recombination between $Q_A^{\bullet-}$ and the donor side of PSII were measured after a single flash (Figure 4). These measurements were conducted at 325 nm, a wavelength where interference from $Y_Z^{\bullet}$ and the Mn cluster is minimal (*77*−*81*). In both wild-type* and D1-H332E PSII particles, the $Q_A^{\bullet-}$ decay kinetics were fit with three exponentially decaying phases[2] (Table 1). The most rapidly decaying phase, with rate constant k_1, was assumed to represent charge recombination between $Q_A^{\bullet-}$ and $Y_Z^{\bullet}$ (*78*, *81*, *82*). This phase had $k_1^{-1} \approx 200$ ms in wild-type* PSII particles and $k_1^{-1} \approx 160$ ms in D1-H332E PSII particles (Table 1). The percentage of reaction centers exhibiting k_1 was 11.4 ± 0.9% in intact wild-type* (Figure 4A), 60 ± 1% in intact D1-H332E (Figure 4B), 63 ± 1% in Mn-depleted wild-type* (Figure 4C), and 66 ± 2% in Mn-depleted D1-H332E (Figure 4D) PSII particles (Table 1).

The percentage of Mn-depleted PSII particles exhibiting k_1 deserves comment. In some Mn-depleted reaction centers, $P_{680}^{\bullet+}$ becomes reduced during the lifetime of $Y_Z^{\bullet}$ by Y_D (*83*), Chl_Z (*62*, *63*), or a carotenoid molecule (*64*, *65*) because of the redox equilibrium, $Y_Z^{\bullet}\ P_{680} \leftrightarrow Y_Z\ P_{680}^{+\bullet}$ (*84*). After the reduction of $P_{680}^{\bullet+}$ in these reaction centers, $Q_A^{\bullet-}$ decays slowly because of the absence of $Y_Z^{\bullet}$ (*78*, *81*, *82*). That a larger percentage of Mn-depleted D1-H332E PSII reaction centers exhibits k_1 than Mn-depleted wild-type* reaction centers may reflect the shorter lifetime of $Y_Z^{\bullet}$ in D1-H332E PSII particles (see below).

The percentage of intact wild-type* PSII particles exhibiting k_1 also deserves comment. In the presence of 0.1−1.0 mM $MnCl_2$, this percentage decreased to 7 ± 1% (not shown, but see Figure 4A). Exogenous Mn^{2+} ions rapidly reduce $Y_Z^{\bullet}$ in PSII particles that lack Mn clusters (*30*, *37*, *85*−*87*) (e.g., see Figures 4C,D), leaving $Q_A^{\bullet-}$ to be oxidized slowly, possibly by charge recombination with the Mn^{3+} ion that remains at the high-affinity Mn binding site. In Mn-depleted

[2] The exponentially decaying phases are reported in terms of initial amplitudes (% of total) and lifetimes (i.e., k^{-1}), that is, the time required for the amplitude to decay to 1/e of its initial value.

Table 1: Kinetics of $Q_A^{\bullet-}$ Decay after a Flash in Intact and Mn-Depleted Wild-Type* and D1-H332E PSII Particles[a]

	k_1		k_2		k_3		reaction centers with Mn clusters (%)
	%	k_1^{-1} (ms)	%	k_2^{-1} (s)	%	k_3^{-1} (s)	
wild-type* (intact)	11.4 ± 0.9	207 ± 34	38 ± 3	3.2 ± 0.4	51 ± 3	26 ± 3	92 ± 3[b]
wild-type* (Mn-depleted)	63 ± 1	190 ± 10	17 ± 1	1.6 ± 0.3	20 ± 1	>100	0[c]
H332E (intact)	60 ± 1	154 ± 12	17 ± 1	2.2 ± 0.3	23 ± 1	80 ± 6	61 ± 5[d]
H332E (intact + $MnCl_2$)	37 ± 1	160 ± 9	32 ± 1	2.5 ± 0.2	31 ± 1	51 ± 4	61 ± 5[d]
H332E (Mn-depleted)	66 ± 2	167 ± 5	17 ± 2	1.8 ± 0.3	17 ± 1	>100	0[c]

[a] Tabulated are the averages and sample standard deviations of 4−10 separate measurements conducted on each sample type. [b] In the presence of 0.1−1.0 mM $MnCl_2$, % k_1 decreased to 7 ± 1%, and 100% of wild-type* reaction centers were assumed to contain Mn clusters or Mn^{2+} ions (see text). [c] Assumed. [d] Calculated from the relation 100 × [(66 − 60) + (37 − 7)]/(66 − 7). Note that the percentage of D1-H332E reaction centers that are photooxidized by a single flash is 100 × (66 − 60)/(66 − 7) = 10 ± 4%. In an additional 51 ± 3% of reaction centers [100 × (37 − 7)/(66 − 7) = 51 ± 3%], Mn clusters that are not photooxidized by a flash protect $Y_Z^{\bullet}$ from reduction by exogenous Mn^{2+} ions (see text).

PSII particles from *Synechocystis* sp. PCC 6803, Mn^{2+} reduces $Y_Z^{\bullet}$ with $K_M = 1\ \mu M$ (*37*). Therefore, 0.1 mM $MnCl_2$ should eliminate k_1 in reaction centers that lack Mn clusters. However, because 7 ± 1% of intact wild-type* PSII particles continue to exhibit k_1 in the presence of 0.1−1.0 mM $MnCl_2$, a small percentage of $Q_A^{\bullet-}$ must recombine with $Y_Z^{\bullet}$ even when the high-affinity Mn binding site near Y_Z is occupied by a Mn cluster or by a Mn^{2+} ion. It is unlikely that this phenomenon is an artifact introduced during isolation of the PSII particles: when charge recombination between $Q_A^{\bullet-}$ and the donor side of PSII is measured in intact wild-type* cells of *Synechocystis* 6803, approximately 16% of the variable fluorescence yield decays[3] with $k_1^{-1} = 100 \pm 40$ ms (*39*) (also see ref *37*). That a small percentage of $Q_A^{\bullet-}$ recombines with $Y_Z^{\bullet}$ despite the presence of a Mn cluster or a Mn^{2+} ion may be caused by heterogeneities or conformational equilibria that slow the reduction of $Y_Z^{\bullet}$ by Mn in a fraction of reaction centers. The microsecond phases of $P_{680}^{\bullet+}$ reduction in intact PSII preparations have been proposed to reflect an equilibrium between different conformational states of PSII (*88*) or between different protonation states of hydrogen-bonded networks leading from Y_Z to the lumenal surface (*89*) (see also the discussion in ref *90*). Such equilibria may contribute to photochemical misses in PSII by allowing $Q_A^{\bullet-}$ to reduce $P_{680}^{\bullet+}$ in the equilibrium population of reaction centers in which electron donation from Y_Z is slow (*88*). However, equilibria that slow the reduction of $Y_Z^{\bullet}$ by Mn in a small percentage of reaction centers probably would not contribute to photochemical misses in vivo because $Q_A^{\bullet-}$ would presumably be oxidized by Q_B before it could reduce $Y_Z^{\bullet}$.

To estimate the percentage of intact wild-type* PSII particles that contain flash-oxidizable Mn clusters, we assume that 0% of Mn-depleted PSII reaction centers contain flash-oxidizable Mn ions and that, in the presence of 0.1 mM $MnCl_2$, 100% of intact wild-type* PSII particles contain flash-oxidizable Mn clusters or Mn^{2+} ions. Because 7 ± 1% of intact wild-type* PSII reaction centers exhibit k_1 in the presence of 0.1−1.0 mM $MnCl_2$ (see above) and 63 ± 1% of Mn-depleted wild-type* PSII reaction centers exhibit k_1 in the absence of added $MnCl_2$ (Table 1), the total dynamic range for k_1 is (63 − 7)%. Therefore, because 11.4 ± 0.9% of intact wild-type* PSII reaction centers exhibit k_1 in the absence of added $MnCl_2$ (Table 1), the percentage of intact wild-type* PSII reaction centers containing flash-oxidizable Mn clusters is 100 × (63 − 11.4)/(63 − 7) = 92 ± 3%.

To estimate the percentage of intact D1-H332E PSII particles that contain flash-oxidizable Mn clusters, we proceed as in the previous paragraph except that, because 66 ± 2% of Mn-depleted D1-H332E PSII reaction centers exhibit k_1 in the absence of $MnCl_2$ (Table 1), the total dynamic range for k_1 is (66 − 7)%. Therefore, because 60 ± 1% of intact D1-H332E PSII reaction centers exhibit k_1 after a flash (Table 1), the percentage of intact D1-H332E PSII reaction centers containing flash-oxidizable Mn clusters is 100 × (66 − 60)/(66 − 7) = 10 ± 4%.

In the previous paragraph, we estimated that only 10 ± 4% of intact D1-H332E PSII particles contain flash-oxidized Mn clusters. However, the integrated area of the multiline EPR signal observed in D1-H332E PSII particles after continuous illumination in the presence of DCMU (Figure 1) shows that approximately 57% of D1-H332E reaction centers contain photooxidizable Mn clusters. The apparent discrepancy between the EPR and optical data suggests that the quantum yield for Mn oxidation is very low in D1-H332E PSII particles. To test this possibility, the kinetics of $Q_A^{\bullet-}$ oxidation in D1-H332E PSII particles were also measured in the presence of 0.1 mM $MnCl_2$ (Figure 4B). Whereas 0.1 mM $MnCl_2$ dramatically slowed the rate of $Q_A^{\bullet-}$ oxidation in both Mn-depleted wild-type* and Mn-depleted D1-H332E PSII particles (Figure 4C,D), the same concentration of exogenous Mn^{2+} ions slowed $Q_A^{\bullet-}$ oxidation in intact D1-H332E PSII particles only moderately (Figure 4B). In intact D1-H332E PSII particles, $Q_A^{\bullet-}$ continued to be oxidized rapidly in 37 ± 1% of reaction centers in the presence of 0.1 mM $MnCl_2$ (Table 1). Evidently, some D1-H332E PSII particles contain Mn clusters that are not photooxidized by a flash but that protect $Y_Z^{\bullet}$ from reduction by exogenous Mn^{2+} ions. In these PSII particles, $Y_Z^{\bullet}$ is rapidly reduced by $Q_A^{\bullet-}$. To estimate the percentage of these PSII particles, we proceed as in the previous paragraph. Because 66 ± 2% of Mn-depleted D1-H332E PSII reaction centers exhibit k_1 in the absence of $MnCl_2$ (Table 1), the total dynamic range for k_1 is (66 − 7)%. Therefore, the percentage of intact D1-H332E reaction centers containing Mn clusters that are not photooxidized by a flash but that protect $Y_Z^{\bullet}$ from reduction is 100 × (37 − 7)/(66 − 7) = 51 ± 3%. Consequently, the total fraction of intact D1-H332E PSII particles containing Mn clusters is 61 ± 5% (i.e., 10 ± 4% plus 51 ± 3%). Of these, 100 × 10/61 = 16 ± 7% reduce $Y_Z^{\bullet}$ after a flash, and the remaining 100 × 51/61 = 84 ± 8% protect $Y_Z^{\bullet}$ from reduction by Mn^{2+} ions. Because 61 ± 5% of intact D1-

[3] At the pH values employed, all kinetic phases of charge recombination are more rapid in intact cells of *Synechocystis* sp. PCC 6803 than in isolated PSII particles (*37*, *38*).

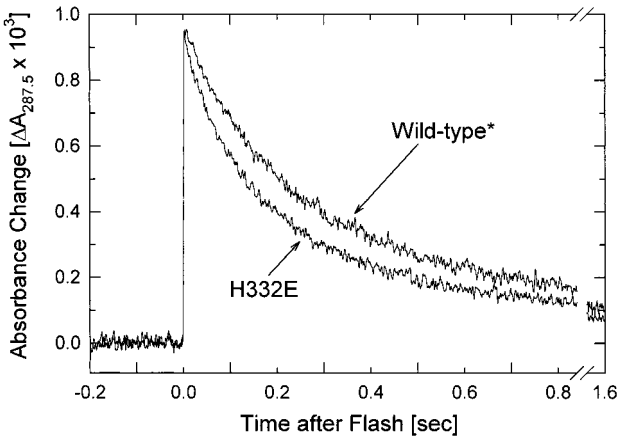

FIGURE 5: Formation and decay of $Y_Z^{\bullet}$ after a single flash applied to Mn-depleted PSII particles, as measured at 287.5 nm. Conditions: same as in Figure 4 but without DCMU or DMSO. Each trace represents the average of 288 sweeps. Samples were replaced after 144 sweeps.

H332E PSII particles contain Mn clusters and approximately 57% of D1-H332E reaction centers give rise to the S_2 state multiline EPR signal (Figure 1), all Mn clusters present in D1-H332E reaction centers appear to be photooxidizable, albeit with a low quantum yield.

Electron-Transfer Kinetics: $Y_Z^{\bullet}$ Reduction by $Q_A^{\bullet-}$. In the absence of exogenous Mn^{2+} ions, the fastest phase of $Q_A^{\bullet-}$ oxidation, k_1, was more rapid in D1-H332E PSII particles than in wild-type* (Figure 4, Table 1). This observation suggests that charge recombination between $Q_A^{\bullet-}$ and $Y_Z^{\bullet}$ is accelerated in D1-H332E compared to wild-type*. To test this possibility, the kinetics of $Y_Z^{\bullet}$ decay in Mn-depleted wild-type* and Mn-depleted D1-H332E PSII particles were measured directly at 287.5 nm, an isosbestic point for $Q_A^{\bullet-}$ in *Synechocystis* sp. PCC 6803 (*81*, *91*). The decay kinetics were fit with two exponentially decaying phases (Figure 5). In Mn-depleted wild-type* PSII particles, 70 ± 4% of $Y_Z^{\bullet}$ decayed with $k^{-1} = 210 \pm 20$ ms, and the remainder decayed with $k^{-1} = 1.5 \pm 0.1$ s. In D1-H332E PSII particles, 70 ± 3% of $Y_Z^{\bullet}$ decayed with $k^{-1} = 150 \pm 5$ ms, and the remainder decayed with $k^{-1} = 1.1 \pm 0.1$ s. These data confirm that charge recombination between $Q_A^{\bullet-}$ and $Y_Z^{\bullet}$ is accelerated in D1-H332E PSII particles in comparison to wild-type*.

DISCUSSION

At least 10 mutations have been constructed at D1-His332 in *Synechocystis* sp. PCC 6803 (*42*, *44*, *45*). None are photoautotrophic. Only the H332Q and H332S mutants evolve O_2, and at only 10−15% the rate of wild-type cells. In all mutants except D1-H332E and D1-H332D, substantial fractions of PSII complexes lack photooxidizable Mn ions in vivo (*45*). These data show that D1-His332 influences the assembly or stability of the Mn cluster. Nevertheless, the high-affinity Mn binding site identified in D1-Asp170 mutants (*37*, *86*) remains intact (*44*). Several D1-His332 mutants are extremely sensitive to photooxidative damage (photoinhibition) (for reviews of photoinhibition in PSII, see refs *92* and *93*), possibly because toxic, activated oxygen species are released from perturbed Mn clusters (*45*). Because Gln and Glu functionally replace His as a ligand to Fe in cytochrome *c* peroxidase (*94*), and because Asp and Ser are potential ligands to Mn, it was proposed that D1-His332 may ligate the Mn cluster and that its redox properties are substantially altered in the Asp and Glu mutants (*45*).

In the current study, we show that the mutation D1-H332E alters the magnetic properties of the Mn cluster and alters the redox properties of both Y_Z and the Mn cluster. On the basis of the kinetics of $Q_A^{\bullet-}$ oxidation in the presence and absence of exogenous Mn^{2+} ions, we estimate that 61 ± 5% of D1-H332E PSII particles retain Mn clusters after isolation. This estimate agrees with that obtained from the integrated area of the S_2 state multiline EPR signal observed in the mutant PSII particles. However, only a minority of these Mn clusters (16 ± 7%) reduce $Y_Z^{\bullet}$ after a flash; the remaining Mn clusters protect $Y_Z^{\bullet}$ from reduction by exogenous Mn^{2+} ions. We propose that this low quantum yield of oxidation of endogenous Mn clusters in D1-H332E PSII particles is caused by a dramatic slowing of the rate of electron transfer from the Mn cluster to $Y_Z^{\bullet}$ during the $S_1 \rightarrow S_2$ transition. The extent of slowing can be estimated. If only $Q_A^{\bullet-}$ and the Mn cluster compete to reduce $Y_Z^{\bullet}$ in D1-H332E PSII particles, then, because $Q_A^{\bullet-}$ reduces $Y_Z^{\bullet}$ with $k^{-1} \approx 160$ ms and only 16 ± 7% of the Mn clusters in D1-H332E PSII particles reduce $Y_Z^{\bullet}$ after a flash, the rate of electron transfer from Mn to $Y_Z^{\bullet}$ during the $S_1 \rightarrow S_2$ transition must have $k^{-1} \approx 0.8$ s. This rate constant is 8000-fold slower than that in wild-type PSII preparations, where $Y_Z^{\bullet}$ oxidizes the S_1 state Mn cluster with a half-time of 55−110 μs (i.e., with $k^{-1} =$ 80−160 μs) (see refs *95*−*98* and references cited therein). Once the S_2 state is formed in the D1-H332E mutant, further oxidation of the Mn cluster by $Y_Z^{\bullet}$ appears blocked, as shown by the accumulation of a $Y_Z^{\bullet}S_2$ "split" EPR signal under multiple turnover conditions (Figure 3). This inhibition is consistent with the inability of D1-H332E cells to evolve O_2 (*45*).

The low quantum yield for the oxidation of assembled Mn clusters in D1-H332E PSII particles raises the possibility that the formation kinetics and stabilities of one or more intermediates formed during photoactivation of the Mn cluster (see refs *99*−*103* and references cited therein) may also be altered in D1-H332E cells, although not sufficiently to prevent cluster assembly. The quantum yield for Mn^{2+} oxidation by $Y_Z^{\bullet}$ in Mn-depleted D1-H332E PSII particles appears to be normal (Figure 4D).

The low quantum yield for oxidation of the Mn cluster (Figure 4), the approximately 100 K higher temperature threshold for forming the S_2 state (Figure 2), and the inability to advance beyond the $Y_Z^{\bullet}S_2$ state (Figure 3) all show that the redox properties of the Mn cluster are dramatically altered in the D1-H332E mutant. The rate of charge recombination between $Q_A^{\bullet-}$ and $Y_Z^{\bullet}$ in Mn-depleted D1-H332E PSII particles was accelerated in comparison to wild-type* (Figure 5). The rate of this reaction is determined by the rate of electron transfer from $Q_A^{\bullet-}$ to $P_{680}^{\bullet+}$ and by the equilibrium, $P_{680}^{\bullet+}\ Y_Z \leftrightarrow P_{680}\ Y_Z^{\bullet}$ (*104*). Although we are unable to exclude an alteration of the redox properties of Q_A or P_{680}, it seems more likely that the accelerated rate of charge recombination between $Q_A^{\bullet-}$ and $Y_Z^{\bullet}$ in Mn-depleted D1-H332E PSII particles represents an alteration of the redox properties of Y_Z.

The absence of an S_1 state parallel-mode multiline EPR signal and the additional hyperfine lines and narrower splittings of the S_2 state multiline EPR signal of D1-H332E

show that the magnetic properties of the Mn clusters in D1-H332E PSII particles are also altered. Altered S_2 state multiline EPR spectra have previously been reported in PSII preparations that have been treated with NH_3 (*17*, *76*, *105*−*109*), that have been depleted of Ca^{2+} in the presence of chelating agents (*57*−*61*), or that have had Sr^{2+} substituted for Ca^{2+} (*110*, *111*). In NH_3-treated PSII preparations, the alterations in the multiline EPR signal are caused by a change in the environment of the Mn cluster: NH_3 exchanges into the coordination sphere of the Mn cluster and may form an amido bridge between two Mn ions or between one Mn ion and one Ca^{2+} ion (*109*). In Ca^{2+}-depleted and Sr^{2+}-substituted PSII preparations, the alterations of the multiline EPR signal may also involve a direct alteration in the environment of the Mn cluster. In Ca^{2+}-depleted PSII preparations, the alterations may be caused by ligation of the Mn cluster by a chelating agent (*61*, *112*). Alternatively, the alterations observed in Ca^{2+}-depleted and Sr^{2+}-substituted PSII preparations could arise from loss or substitution of the Ca^{2+} ion that has been proposed to be linked to the Mn cluster by a carboxylato bridge (*36*). However, EXAFS data are contradictory about whether Ca^{2+} is located sufficiently close to the Mn cluster to form such a bridge (e.g., see ref *113* versus ref *114*).

Mutations at D1-His332 appear to diminish the affinity of PSII for Ca^{2+} (*45*). Indeed, isolated D1-H332E PSII particles resemble Ca^{2+}-depleted PSII preparations in that both exhibit altered S_2 state multiline EPR signals, both require higher temperatures to form the S_2 state, both exhibit $S_2Y_Z^{\bullet}$ "split" EPR signals under multiple-turnover conditions, and neither evolves O_2. However, observation of the S_2 state multiline EPR signal in Ca^{2+}-depleted PSII preparations requires the presence of chelating agents (*61*, *112*), whereas no chelating agents were present in the D1-H332E PSII samples. Furthermore, the S_2 state in Ca^{2+}-depleted PSII preparations forms with normal quantum yield (*55*) and is stable for hours at room temperature (*57*−*59*, *61*), whereas the S_2 state in D1-H332E PSII particles forms with very low quantum yield and appears to exhibit normal stability. Furthermore, the D1-H332E PSII particles were analyzed in the presence of 20 mM Ca^{2+}. Therefore, the altered magnetic and redox properties of the Mn clusters in D1-H332E PSII particles reflect more than simply a loss of Ca^{2+} ions. Indeed, the higher temperature threshold for forming the S_2 state is also characteristic of PSII preparations that have been treated with acetate (*54*). Acetate-treated PSII preparations are also unable to advance beyond the $S_2Y_Z^{\bullet}$ state (*17*, *54*, *70*−*73*) and give rise to an S_2 state multiline EPR signal only under special circumstances (*54*, *115*). Acetate binds competitively with Cl^- (*116*) to a site located close to Y_Z (*72*) and possibly located directly on the Mn cluster (*72*). Chloride-depleted PSII preparations are also unable to advance beyond the $S_2Y_Z^{\bullet}$ state (*68*, *69*, *117*, *118*).

That acetate-inhibited, Ca^{2+}-depleted, Cl^--depleted, and D1-H332E mutant PSII preparations are all unable to advance beyond the $S_2Y_Z^{\bullet}$ state suggests a mechanism for the inhibition of Mn oxidation in D1-His332E PSII particles. Both acetate-treatment (*80*, *119*) and Ca^{2+}-depletion (*68*, *120*) dramatically slow the oxidation of Y_Z by $P_{680}^{+\bullet}$, as is observed in D1-His190 mutants, where the hydrogen-bonding properties of Y_Z are disrupted (*41*−*44*, *50*, *90*, *121*−*124*). Consequently, both acetate-treatment and Ca^{2+}-depletion are believed to disrupt a network of hydrogen bonds that includes Y_Z and D1-His190 (*89*, *90*, *120*). To provide the necessary driving force for oxidizing the Mn cluster, $Y_Z^{\bullet}$ is believed to abstract both an electron and a proton from the Mn cluster in its S_2 and S_3 states (*4*, *18*−*23*, *54*). Acetate-treatment, Ca^{2+}-depletion, and Cl^--depletion have all been proposed to block the conversion of $S_2Y_Z^{\bullet}$ to S_3Y_Z by inhibiting proton transfer from Mn to $Y_Z^{\bullet}$: these treatments are proposed to disrupt the network of hydrogen bonds that connects Y_Z with the water-deprived Mn ligands from which the proton is abstracted (*22*, *54*, *116*). A similar disruption of these hydrogen bonds may occur in the D1-H332E mutant. For example, if D1-His332 is a ligand of the Mn cluster, replacing this residue with a potentially bidentate carboxylate group could prevent the binding of a substrate water molecule or otherwise perturb the network of hydrogen bonds in a manner similar to the binding of acetate.[4]

The altered properties of both the Mn cluster and Y_Z in D1-H332E PSII particles are consistent with D1-His332 being located close to the Y_Z−Mn complex. They are also consistent with the possibility that D1-His332 is a ligand of the Mn cluster. Studies are underway to determine if the nitrogen couplings observed in the ESEEM spectrum of the wild-type S_2 state multiline EPR signal (*34*) are diminished in D1-H332E PSII particles, as would be expected if D1-His332 ligates the Mn cluster.

[4] This specific scenario was suggested by a reviewer.

ACKNOWLEDGMENT

We are grateful to A. P. Nguyen for maintaining the wild-type* and mutant cultures of *Synechocystis* 6803 and for help isolating some of the PSII particles. We also thank the reviewers for helpful comments on the manuscript.

REFERENCES

1. Rhee, K. H., Morris, E. P., Barber, J., and Kühlbrandt, W. (1998) *Nature 396*, 283−286.
2. Hankamer, B., Morris, E. P., and Barber, J. (1999) *Nat. Struct. Biol. 6*, 560−564.
3. Debus, R. J. (1992) *Biochim. Biophys. Acta 1102*, 269−352.
4. Britt, R. D. (1996) in *Oxygenic Photosynthesis: The Light Reactions* (Ort, D. R., and Yocum, C. F., Eds.) pp 137−164, Kluwer Academic Publishers, Dordrecht, The Netherlands.
5. Diner, B. A., and Babcock, G. T. (1996) in *Oxygenic Photosynthesis: The Light Reactions* (Ort, D. R., and Yocum, C. F., Eds.) pp 213−247, Kluwer Academic Publishers, Dordrecht, The Netherlands.
6. Yachandra, V. K., Sauer, K., and Klein, M. P. (1996) *Chem. Rev. 96*, 2927−2950.
7. Renger, G. (1997) *Physiol. Plant. 100*, 828−841.
8. Penner-Hahn, J. E. (1998) *Struct. Bonding 90*, 1−36.
9. Hoganson, C. W., and Babcock, G. T. (2000) in *Metal Ions in Biological Systems* (Sigel, A., and Sigel, H., Eds.) Vol. 37, pp 613−656, Marcel Dekker, New York.
10. Debus, R. J. (2000) in *Metal Ions in Biological Systems* (Sigel, A., and Sigel, H., Eds.) Vol. 37, pp 657−710, Marcel Dekker, New York.
11. Randall, D. W., Sturgeon, B. E., Ball, J. A., Lorigan, G. A., Chan, M. K., Klein, M. P., Armstrong, W. H., and Britt, R. D. (1995) *J. Am. Chem. Soc. 117*, 11780−11789.
12. Peloquin, J. M., Campbell, K. A., and Britt, R. D. (1998) *J. Am. Chem. Soc. 120*, 6840−6841.

13. Roelofs, T. A., Liang, W., Latimer, M. J., Cinco, R. M., Rompel, A., Andrews, J. C., Sauer, K., Yachandra, V. K., and Klein, M. P. (1996) *Proc. Natl. Acad. Sci. U.S.A. 93*, 3335−3340.
14. Iuzzolino, L., Dittmer, J., Dörner, W., Meyer-Klaucke, W., and Dau, H. (1998) *Biochemistry 37*, 17112−17119.
15. Dorlet, P., Di Valentin, M., Babcock, G. T., and McCracken, J. L. (1998) *J. Phys. Chem. B 102*, 8239−8247.
16. Lakshmi, K. V., Eaton, S. S., Eaton, G. R., Frank, H. A., and Brudvig, G. W. (1998) *J. Phys. Chem. B 102*, 8327−8335.
17. MacLachlan, D. J., Nugent, J. H. A., Warden, J. T., and Evans, M. C. W. (1994) *Biochim. Biophys. Acta 1188*, 325−334.
18. Hoganson, C. W., Lydakis-Simantiris, N., Tang, X.-S., Tommos, C., Warncke, K., Babcock, G. T., Diner, B. A., McCracken, J., and Styring, S. (1995) *Photosynth. Res. 46*, 177−184.
19. Hoganson, C. W., and Babcock, G. T. (1997) *Science 277*, 1953−1956.
20. Tommos, C., and Babcock, G. T. (1998) *Acc. Chem. Res. 31*, 18−25.
21. Tommos, C., Hoganson, C. W., Di Valentin, M., Lydakis-Simantiris, N., Dorlet, P., Westphal, K., Chu, H.-A., McCracken, J., and Babcock, G. T. (1998) *Curr. Opin. Chem. Biol. 2*, 244−252.
22. Limburg, J., Szalai, V. A., and Brudvig, G. W. (1999) *J. Chem. Soc., Dalton Trans.*, 1353−1361.
23. Gilchrist, M. L., Jr., Ball, J. A., Randall, D. W., and Britt, R. D. (1995) *Proc. Natl. Acad. Sci. U.S.A. 92*, 9545−9549.
24. Britt, R. D., Peloquin, J. M., and Campbell, K. A. (2000) *Annu. Rev. Biophys. Biomol. Struct.* (in press).
25. Tamura, N., Ikeuchi, M., and Inoue, Y. (1989) *Biochim. Biophys. Acta 973*, 281−289.
26. Seibert, M., Tamura, N., and Inoue, Y. (1989) *Biochim. Biophys. Acta 974*, 185−191.
27. Preston, C., and Seibert, M. (1991) *Biochemistry 30*, 9615−9624.
28. Preston, C., and Seibert, M. (1991) *Biochemistry 30*, 9625−9633.
29. Blubaugh, D. J., and Cheniae, G. M. (1992) in *Research in Photosynthesis* (Murata, N., Ed.) Vol. II, pp 361−364, Kluwer Academic Publishers, Dordrecht, The Netherlands.
30. Magnuson, A., and Andréasson, L.-E. (1997) *Biochemistry 36*, 3254−3261.
31. Tamura, N., Noda, K., Wakamatsu, K., Kamachi, H., Inoue, H., and Wada, K. (1997) *Plant Cell Physiol. 38*, 578−585.
32. Ghirardi, M. L., Lutton, T. W., and Seibert, M. (1998) *Biochemistry 37*, 13559−13566.
33. Ghirardi, M. L., Preston, C., and Seibert, M. (1998) *Biochemistry 37*, 13567−13574.
34. Tang, X.-S., Diner, B. A., Larsen, B. S., Gilchrist, M. L., Jr., Lorigan, G. A., and Britt, R. D. (1994) *Proc. Natl. Acad. Sci. U.S.A. 91*, 704−708.
35. Noguchi, T., Inoue, Y., and Tang, X.-S. (1999) *Biochemistry 38*, 10187−10195.
36. Noguchi, T., Ono, T.-A., and Inoue, Y. (1995) *Biochim. Biophys. Acta 1228*, 189−200.
37. Nixon, P. J., and Diner, B. A. (1992) *Biochemistry 31*, 942−948.
38. Boerner, R. J., Nguyen, A. P., Barry, B. A., and Debus, R. J. (1992) *Biochemistry 31*, 6660−6672.
39. Chu, H.-A., Nguyen, A. P., and Debus, R. J. (1994) *Biochemistry 33*, 6137−6149.
40. Whitelegge, J. P., Koo, D., Diner, B. A., Domian, I., and Erickson, J. M. (1995) *J. Biol. Chem. 270*, 225−235.
41. Chu, H.-A., Nguyen, A. P., and Debus, R. J. (1995) *Biochemistry 34*, 5839−5858.
42. Nixon, P. J., Chisholm, D. A., and Diner, B. A. (1992) in *Plant Protein Engineering* (Shewry, P., and Gutteridge, S., Eds.) pp 93−141, Cambridge University Press, Cambridge, United Kingdom.
43. Roffey, R. A., Kramer, D. M., Govindjee, and Sayre, R. T. (1994) *Biochim. Biophys. Acta 1185*, 257−270.
44. Nixon, P. J., and Diner, B. A. (1994) *Biochem. Soc. Trans. 22*, 338−343.
45. Chu, H.-A., Nguyen, A. P., and Debus, R. J. (1995) *Biochemistry 34*, 5859−5882.
46. Nixon, P. J., Trost, J. T., and Diner, B. A. (1992) *Biochemistry 31*, 10859−10871.
47. Chu, H.-A., Nguyen, A. P., and Debus, R. J. (1995) in *Photosynthesis: From Light to Biosphere* (Mathis, P., Ed.) Vol. II, pp 439−442, Kluwer Academic Publishers, Dordrecht, The Netherlands.
48. Williams, J. G. K. (1988) *Methods Enzymol. 167*, 766−778.
49. Vermaas, W. F. J. (1994) *Biochim. Biophys. Acta 1187*, 181−186.
50. Hays, A.-M. A., Vassiliev, I. R., Golbeck, J. H., and Debus, R. J. (1998) *Biochemistry 37*, 11352−11365.
51. Tang, X.-S., and Diner, B. A. (1994) *Biochemistry 33*, 4594−4603.
52. de Paula, J. C., Innes, J. B., and Brudvig, G. W. (1985) *Biochemistry 24*, 8114−8120.
53. Styring, S., and Rutherford, A. W. (1988) *Biochim. Biophys. Acta 933*, 378−387.
54. Szalai, V. A., and Brudvig, G. W. (1996) *Biochemistry 35*, 15080−15087.
55. Ono, T.-A., and Inoue, Y. (1990) *Biochim. Biophys. Acta 1015*, 373−377.
56. Ono, T.-A., Kusunoki, M., Matsushita, T., Oyanagi, H., and Inoue, Y. (1991) *Biochemistry 30*, 6836−6841.
57. Boussac, A., Zimmermann, J.-L., and Rutherford, A. W. (1989) *Biochemistry 28*, 8984−8989.
58. Sivaraja, M., Tso, J., and Dismukes, G. C. (1989) *Biochemistry 28*, 9459−9464.
59. Ono, T.-A., and Inoue, Y. (1990) *Biochim. Biophys. Acta 1020*, 269−277.
60. Boussac, A., Zimmermann, J.-L., Rutherford, A. W., and Lavergne, J. (1990) *Nature 347*, 303−306.
61. Boussac, A., Zimmermann, J.-L., and Rutherford, A. W. (1990) *FEBS Lett. 277*, 69−74.
62. Thompson, L. K., and Brudvig, G. W. (1988) *Biochemistry 27*, 6653−6658.
63. Stewart, D. H., Cua, A., Chisholm, D. A., Diner, B. A., Bocian, D. F., and Brudvig, G. W. (1998) *Biochemistry 37*, 10040−10046.
64. Hanley, J., Deligiannakis, Y., Pascal, A. A., Faller, P., and Rutherford, A. W. (1999) *Biochemistry 38*, 8189−8195.
65. Vrettos, J. S., Stewart, D. H., de Paula, J. C., and Brudvig, G. W. (1999) *J. Phys. Chem. B 103*, 6403−6406.
66. Campbell, K. A., Peloquin, J. M., Pham, D. P., Debus, R. J., and Britt, R. D. (1998) *J. Am. Chem. Soc. 120*, 447−448.
67. Campbell, K. A., Gregor, W., Pham, D. P., Peloquin, J. M., Debus, R. J., and Britt, R. D. (1998) *Biochemistry 37*, 5039−5045.
68. Boussac, A., Sétif, P., and Rutherford, A. W. (1992) *Biochemistry 31*, 1224−1234.
69. Baumgarten, M., Philo, J. S., and Dismukes, G. C. (1990) *Biochemistry 29*, 10814−10822.
70. MacLachlan, D. J., and Nugent, J. H. A. (1993) *Biochemistry 32*, 9772−9780.
71. Szalai, V. A., and Brudvig, G. W. (1996) *Biochemistry 35*, 1946−1953.
72. Force, D. A., Randall, D. W., and Britt, R. D. (1997) *Biochemistry 36*, 12062−12070.
73. Tang, X.-S., Randall, D. W., Force, D. A., Diner, B. A., and Britt, R. D. (1996) *J. Am. Chem. Soc. 118*, 7638−7639.
74. Andréasson, L.-E., and Lindberg, K. (1992) *Biochim. Biophys. Acta 1100*, 177−183.
75. Hallahan, B. J., Nugent, J. H. A., Warden, J. T., and Evans, M. C. W. (1992) *Biochemistry 31*, 4562−4573.
76. Boussac, A., Rutherford, A. W., and Styring, S. (1990) *Biochemistry 29*, 24−32.
77. van Gorkom, H. J. (1974) *Biochim. Biophys. Acta 347*, 439−442.
78. Dekker, J. P., van Gorkom, H. J., Brok, M., and Ouwehand, L. (1984) *Biochim. Biophys. Acta 764*, 301−309.
79. Schatz, G. H., and van Gorkom, H. J. (1985) *Biochim. Biophys. Acta 810*, 283−294.

80. Gerken, S., Dekker, J. P., Schlodder, E., and Witt, H. T. (1989) *Biochim. Biophys. Acta 977*, 52−61.
81. Metz, J. G., Nixon, P. J., Rögner, M., Brudvig, G. W., and Diner, B. A. (1989) *Biochemistry 28*, 6960−6969.
82. Rappaport, F., and Lavergne, J. (1997) *Biochemistry 36*, 15294−15302.
83. Buser, C. A., Thompson, L. K., Diner, B. A., and Brudvig, G. W. (1990) *Biochemistry 29*, 8977−8985.
84. Stewart, D. H., and Brudvig, G. W. (1998) *Biochim. Biophys. Acta 1367*, 63−87.
85. Hoganson, C. W., Ghanotakis, D. F., Babcock, G. T., and Yocum, C. F. (1989) *Photosynth. Res. 22*, 285−293.
86. Diner, B. A., and Nixon, P. J. (1992) *Biochim. Biophys. Acta 1101*, 134−138.
87. Ono, T.-A., and Mino, H. (1999) *Biochemistry 38*, 8778−8785.
88. Lavergne, J., and Rappaport, F. (1998) *Biochemistry 37*, 7899−7906.
89. Tommos, C., and Babcock, G. T. (1999) *Biochim. Biophys. Acta* (in press).
90. Hays, A.-M. A., Vassiliev, I. R., Golbeck, J. H., and Debus, R. J. (1999) *Biochemistry 38*, 11851−11865.
91. Debus, R. J., Campbell, K. A., Pham, D. P., Hays, A.-M. A., Peloquin, J. M., and Britt, R. D. (1998) in *Photosynthesis: Mechanisms and Effects* (Garab, G., Ed.) Vol. II, pp 1375−1378, Kluwer Academic Publishers, Dordrecht, The Netherlands.
92. Aro, E.-M., Virgin, I., and Andersson, B. (1993) *Biochim. Biophys. Acta 1143*, 113−134.
93. Andersson, B., and Barber, J. (1996) in *Photosynthesis and the Environment* (Baker, N. R., Ed.) pp 101−121, Kluwer Academic Publishers, Dordrecht, The Netherlands.
94. Choudhury, K., Sundaramoorthy, M., Hickman, A., Yonetani, T., Woehl, E., Dunn, M. F., and Poulos, T. L. (1994) *J. Biol. Chem. 269*, 20239−20249.
95. van Leeuwen, P. J., Heimann, C., Gast, P., Dekker, J. P., and van Gorkom, H. J. (1993) *Photosynth. Res. 38*, 169−176.
96. Rappaport, F., Blanchard-Desce, M., and Lavergne, J. (1994) *Biochim. Biophys. Acta 1184*, 178−192.
97. Razeghifard, M. R., Klughammer, C., and Pace, R. J. (1997) *Biochemistry 36*, 86−92.
98. Razeghifard, M. R., and Pace, R. J. (1997) *Biochim. Biophys. Acta 1322*, 141−150.
99. Chen, C., Kazimir, J., and Cheniae, G. M. (1995) *Biochemistry 34*, 13511−13526.
100. Burnap, R. L., Qian, M., and Pierce, C. (1996) *Biochemistry 35*, 874−882.
101. Ananyev, G. M., and Dismukes, G. C. (1996) *Biochemistry 35*, 4102−4109.
102. Ananyev, G. M., and Dismukes, G. C. (1996) *Biochemistry 35*, 14608−14617.
103. Zaltsman, L., Ananyev, G. M., Bruntrager, E., and Dismukes, G. C. (1997) *Biochemistry 36*, 8914−8922.
104. Diner, B. A. (1998) *Methods Enzymol. 297*, 337−360.
105. Beck, W. F., and Brudvig, G. W. (1986) *Biochemistry 25*, 6479−6486.
106. Beck, W. F., de Paula, J. C., and Brudvig, G. W. (1986) *J. Am. Chem. Soc. 108*, 4018−4022.
107. Aasa, R., Andréasson, L.-E., Lagenfelt, G., and Vänngård, T. (1987) *FEBS Lett. 221*, 245−248.
108. Andréasson, L.-E., Hansson, Ö., and von Schenck, K. (1988) *Biochim. Biophys. Acta 936*, 351−360.
109. Britt, R. D., Zimmermann, J.-L., Sauer, K., and Klein, M. P. (1989) *J. Am. Chem. Soc. 111*, 3522−3532.
110. Boussac, A., and Rutherford, A. W. (1988) *Biochemistry 27*, 3476−3483.
111. Ono, T.-A., and Inoue, Y. (1989) *Arch. Biochem. Biophys. 275*, 440−448.
112. Zimmermann, J.-L., Boussac, A., and Rutherford, A. W. (1993) *Biochemistry 32*, 4831−4841.
113. Cinco, R. M., Robblee, J. H., Rompel, A., Fernandez, C., Yachandra, V. K., Sauer, K., and Klein, M. P. (1998) *J. Phys. Chem. B 102*, 8248−8256.
114. Riggs-Gelasco, P. J., Mei, R., Ghanotakis, D. F., Yocum, C. F., and Penner-Hahn, J. E. (1996) *J. Am. Chem. Soc. 118*, 2400−2410.
115. Szalai, V. A., Kühne, H., Lakshmi, K. V., and Brudvig, G. W. (1998) *Biochemistry 37*, 13594−13603.
116. Kühne, H., Szalai, V. A., and Brudvig, G. W. (1999) *Biochemistry 38*, 6604−6613.
117. Ono, T.-A., Noguchi, T., Inoue, Y., Kusunoki, M., Yamaguchi, H., and Oyanagi, H. (1995) *J. Am. Chem. Soc. 117*, 6386−6387.
118. Wincencjusz, H., van Gorkom, H. J., and Yocum, C. F. (1997) *Biochemistry 36*, 3663−3670.
119. Saygin, Ö., Gerken, S., Meyer, B., and Witt, H. T. (1986) *Photosynth. Res. 9*, 71−78.
120. Haumann, M., and Junge, W. (1999) *Biochim. Biophys. Acta 1411*, 121−133.
121. Diner, B. A., Nixon, P. J., and Farchaus, J. W. (1991) *Curr. Opin. Struct. Biol. 1*, 546−554.
122. Roffey, R. A., van Wijk, K. J., Sayre, R. T., and Styring, S. (1994) *J. Biol. Chem. 269*, 5115−5121.
123. Mamedov, F., Sayre, R. T., and Styring, S. (1998) *Biochemistry 37*, 14245−14256.
124. Diner, B. A., and Nixon, P. J. (1998) in *Photosynthesis: Mechanisms and Effects* (Garab, G., Ed.) Vol. II, pp 1177−1180, Kluwer Academic Publishers, Dordrecht, The Netherlands.
125. Boussac, A., Zimmermann, J.-L., Rutherford, A. W., and Lavergne, J. (1990) *Nature 347*, 303−306.

BI9917737